Organic & Biomolecular Chemistry

Dynamic Article Links

Cite this: *Org. Biomol. Chem.*, 2012, **10**, 267

www.rsc.org/obc

PAPER

6-Hydroxyindole-based borondipyrromethene: Synthesis and spectroscopic studies†

Chunchang Zhao,* Peng Feng, Jian Cao, Yulin Zhang, Xuzhe Wang, Yang Yang, Yanfen Zhang and Jinxin Zhang

Received 19th July 2011, Accepted 29th September 2011
DOI: 10.1039/c1ob06200j

A 6-hydroxyindole-based BODIPY, named **BODIPY–OH**, with distinct spectroscopic characteristics is reported. Through a systematic study of the spectroscopic characteristics of **BODIPY–OH** and **BODIPY–O**$^-$ in various solvents containing an organic base, we found that the light-color of the fluorophore can be tuned over a wide range by changing the polarity of solvent/base combinations. The absorption color of the solution can be tuned over a range of 100 nm and the emission color within a wide range from 571 to 681 nm by simply converting the phenol form of **BODIPY–OH** to the phenolate form. Fluorescence of **BODIPY–O**$^-$ with high quantum yield shows relatively large Stokes shift in solvent/base combinations, which are ascribed to the excited state deprotonation from (**BODIPY–OH**)* to (**BODIPY–O**$^-$)*, followed by emission from the ion form.

Introduction

Borondipyrromethene (BODIPY) fluorescent dyes are of high interest as fluorophores due to their valuable photophysical properties, such as high photo- and chemostability, high fluorescence quantum yields, relatively high absorption coefficients, and sharp absorption and fluorescence emission spectra.[1] BODIPYs are well known to show strong emission of wavelengths over 500 nm, their fluorescence is unaffected by solvent polarity and pH, and their fluorescence emission spectra display a slight Stokes shift.[2] However, to finely tune the wavelength of BODIPYs over a wide range including the NIR region, chemical modification approaches should be attempted and the synthesis is usually tedious and non-trivial.[3] Moreover, a small Stokes shift can cause self-quenching and measurement error by excitation interference, which can decrease the detection sensitivity to a great extent.[4] Therefore, dyes with a larger Stokes shift are very promising for fluorescence bioassays. To date, the strategy to design BODIPYs with a relatively large Stokes shift is rarely investigated.

Herein, we report a carefully designed BODIPY named **BODIPY–OH** with straightforward phenol/phenolate interconversion to overcome these deficiencies. The basis of employing **BODIPY–OH** to achieve tunable light-color and relatively large Stokes shift characteristic comes from bioluminescence, a natural phenomenon, which converts chemical energy into light through biochemical production of excited states from ground-state reactants. Fireflies and their analogous beetles, the most studied bioluminescent reaction systems, generate light over a wide range of colors from green to red (emission maxima $\lambda = 530$–640 nm).[5–7] To explain the multicolor bioluminescence of fireflies and their analogous beetles as well as the biochemical origin of the light emission, a vast amount of experimental and model studies have been developed.[8–9] All these studies demonstrate that the phenol–phenolate equilibrium of oxyluciferin, a common bioluminescence center, plays a critical role in varying the emission color; the emission color can be tuned within a wide spectral range from 541 nm to 640 nm by varying only the solvent polarity and the nature of interaction between the phenolate ion and the countercation.[10–11] Motivated by these observations, the research discussed here explores an approach that **BODIPY–OH** with straightforward phenol/phenolate interconversion is judiciously designed and synthesized by the fusion of 6-hydroxyindole moiety to the parent structure of BODIPYs to extend the π-conjugation. **Note** examples of BODIPYs bearing phenolic subunits at position 3, 5, or 8 are found in the literature.[2a,3c,12] However, all show deprotonation dependent fluorescence due to charge transfer from the phenolate to the excited-state BODIPY moiety. In sharp contrast, the **BODIPY–OH** designed here displays a spectral shift and a fine-tuning of the spectra wavelength achieved simply by controlling phenol/phenolate interconversion of the chromophore. More importantly, both **BODIPY–OH** and **BODIPY–O**$^-$ (deprotonation state) display emissions with high quantum yield in solvents. In addition, the fluorescence spectra show relatively large Stokes shifts in solvents in the presence of organic base, obtained by the excited state proton transfer, with (**BODIPY–OH**)* conversion to (**BODIPY–O**$^-$)*, followed by emission from the ion.

Key Laboratory for Advanced Materials and Institute of Fine Chemicals, East China University of Science & Technology, Shanghai, 200237, P. R. China. E-mail: zhaocchang@ecust.edu.cn

† Electronic supplementary information (ESI) available: A detailed description of absorption and emission spectra, HRMS spectra and NMR spectra. See DOI: 10.1039/c1ob06200j

Results and discussion

Synthesis

BODIPY–OH was obtained easily by routine BODIPY formation, using a three-step procedure *via* condensation of 2,4-dimethyl-3-ethylpyrrole with 2-benzoyl-3-methyl-6-methoxyindole followed by removal of the methoxy protecting groups (BBr_3, CH_2Cl_2) and boron insertion with $BF_3{\cdot}OEt_2$ (Scheme 1). The overall yield is 53% for three steps. The methyl ether derivative **BODIPY–OMe** was also obtained in a one-pot, two-step procedure *via* condensation of 2,4-dimethyl-3-ethylpyrrole with 2-benzoyl-3-methyl-6-methoxyindole followed by treatment with $BF_3{\cdot}OEt_2$ (Scheme 1). The structure was fully characterized by ^{1}H NMR, ^{13}C NMR, and HRMS analysis.

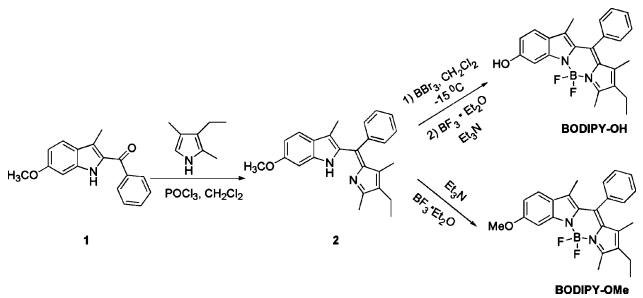

Scheme 1 Synthesis of BODIPY–OH and BODIPY–OMe.

Spectroscopic Properties of BODIPY–OH and BODIPY–OMe

Spectroscopic evaluation of **BODIPY–OH** and its methyl ether derivative **BODIPY–OMe** was performed in several solvents of varying polarity (Table 1, Figure S1, Figure S2, Table S1 and S2 in supporting information). The optical features are characteristics of the BODIPY platform. As is evident from Table 1, Figure S1, S2 and Table S1, S2, the main absorption band of **BODIPY–OH**, attributed to the 0-0 vibrational band of a strong S_0–S_1 transition, is centered between 545 and 563 nm in the pure solvents, while that of **BODIPY–OMe** centered between 544 and 555 nm. The S_0–S_1 absorption band shows minor solvent-dependent variation and the maximum shifts of the absorbance are only 18 nm and 11 nm for **BODIPY–OH** and **BODIPY–OMe** respectively, indicating a weak charge transfer character for the lowest electronic excitation in the ground-state geometry. Similar to the absorption spectra, their emission spectra also show minor solvent-dependent shift. The maximum emission wavelength of **BODIPY–OH** is in 571–583 nm range, while that of **BODIPY–OMe** centered between 567 and 573 nm.

In DMSO, however, a red-shifted absorption band of phenolate anion **BODIPY–O$^-$** (see discussion below) at 644 nm accompanies the original neutral one at 558 nm. A shoulder centered at approximately 606 nm can also be observed, which is assigned to the 0–1 vibrational band of S_0–S_1 transition of **BODIPY–O$^-$**. Similar, the phenol group of **BODIPY–OH** can be partially deprotonated from the excited state upon excitation at 558 nm, therefore two emission bands are generated at *ca.* 583 nm and 680 nm. The shorter emission band comes from the neutral phenol form, while the longer one can be assigned as the emission of **BODIPY–O$^-$** with a large Stokes shift ~120 nm. Upon excitation at 644 nm into the absorption band of **BODIPY–O$^-$**, only one emission from **BODIPY–O$^-$** at 680 nm is observed. These experimental observations imply that a spectral red shift could be achieved by simply controlling the conversion of **BODIPY–OH** from phenol form to phenolate form.

The deprotonation process of **BODIPY–OH** can be observed in UV-vis and fluorescence titration experiments with varying pH (Fig. 1). Increasing pH value from acidic to basic condition, a decrease in the absorption band at 541 nm and a concomitant increase of a new band at 612 nm were observed, with a distinct isosbestic point at 559 nm. In the same way as the absorption spectra, when **BODIPY–OH** was excited at the wavelength of the absorption isosbestic point, the fluorescence spectra of **BODIPY–OH** exhibited phenol/phenolate dependant blue-red switching, as shown in Fig. 1. Increasing the pH value from 7.8 to 10, the spectrum showed a decrease of the emission band at 575 nm and a simultaneous increase of the emission band at 644 nm. The likely characteristic isoemission point at 621 nm makes **BODIPY–OH** an excellent ratiometric pH indicator.

The *K*a values of **BODIPY–OH** were determined by fluorimetric titration as a function of pH using the fluorescence emission spectra. Nonlinear curve fitting of eqn (1) to the fluorescence data *F* recorded as a function of pH yielded values of *K*a, where F_{min} and F_{max} are the fluorescence intensity at minimal and maximal [H$^+$], respectively, and *n* is the number of H$^+$ dissociating from one **BODIPY–OH** dye. In a DMSO-H_2O mixture (1 : 1), the pK_a value is determined to be 9.5.

$$F = \frac{F_{max}[H^+]^n + F_{min}K_a}{[H^+]^n + K_a} \quad (1)$$

Table 1 Spectroscopic data for **BODIPY–OH** and **BODIPY–O$^-$** in various solvents in the absence or presence of organic base (DBU)

Solvent	E_T(N)	λ_{abs} (nm)		λ_{em} (nm)[Φ_F]		
		–OH	**–OMe**	**–OH**	**–O$^-$**(**–OH**+DBN)	**–OMe**
Water	1.000	546	551		629[0.18]	
Methanol	0.762	548	544	577 [0.25]	642 [0.22]	567
Acetonitrile	0.460	542	540	571 [0.22]	664 [0.17]	567
DMSO	0.444	558 644	546	583, 680 [0.34]	675 [0.18]	574
Dichloromethane	0.309	545	546	577 [0.30]	656 [0.24]	571
Toluene	0.099	563	555	586 [0.40]	655 [0.24]	573

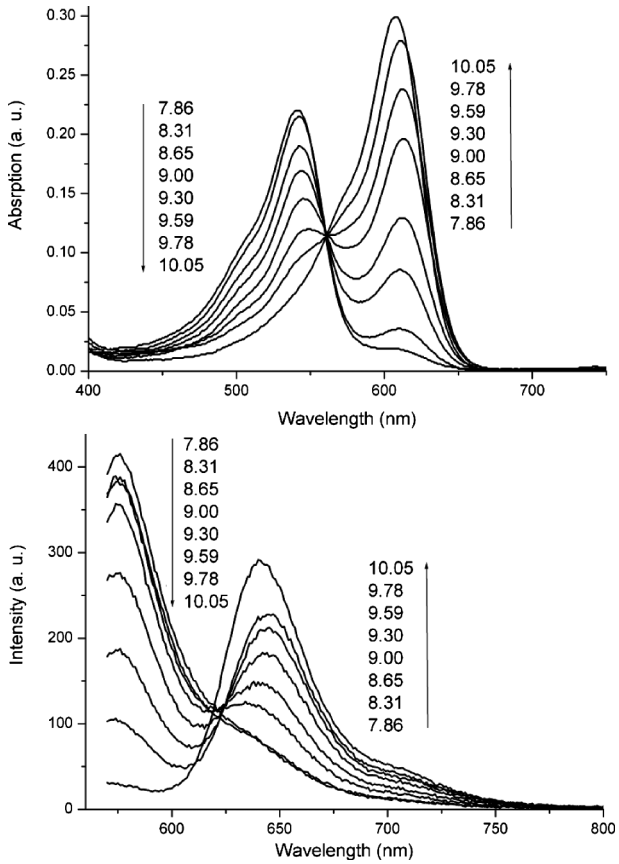

Fig. 1 Absorption spectra (top) of **BODIPY–OH** in buffer solution as a function of pH. Corresponding emission spectra (bottom) (λex = 559 nm). pH was adjusted by NaH_2PO_4 and Na_2HPO_4.

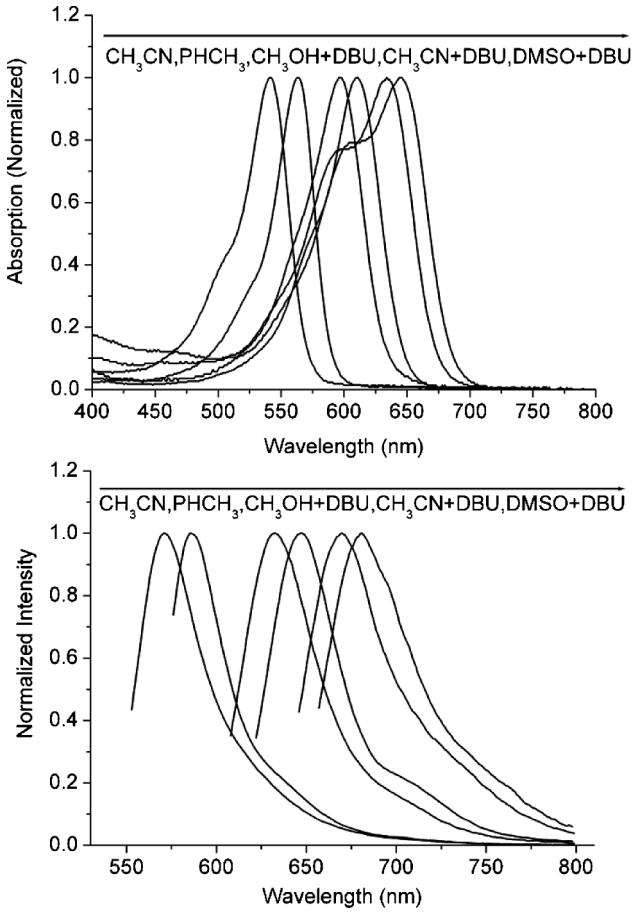

Fig. 2 Normalized absorption (top) and fluorescence emission (bottom) spectra of **BODIPY–OH** in solutions with varying solvent/base combinations. Base: 1,8-diazabicyclo[5.4.0]undec-7-ene (DBU).

The acidity constant in the excited state, pK_a*, can be obtained from the "Förster cycle"[13] according to

$$pK - pK^* = \frac{E_{OH} - E_{O^-}}{2.303RT} \quad (2)$$

where E_{OH} and E_{O}- are the energies of the electronic transitions for **BODIPY–OH** and **BODIPY–O**$^-$, determined as the 0-0 transition energies. These can be estimated by determining the wave number corresponding to the intersection point of the normalized absorption and emission spectra. The pK_a* thus obtained is 5.3 in a DMSO-H_2O mixture (1 : 1).

Spectroscopic properties of deprotonated BODIPY–OH

The optical properties of **BODIPY–OH** in base/solvent systems (Fig. 2) indicate a significant spectral red-shift by varying only the solvent polarity and base/solvent combinations from acetonitrile to CH_3CN/DBU (1,8-diazabicyclo[5.4.0]undec-7-ene) combination, emission spectral maxima range from 571 nm to 681 nm, while the absorption maxima range from 542 nm to 645 nm.

To elucidate the light-color modulation of **BODIPY–OH** by varying solvent/base combinations, measurements of the spectroscopic properties of the phenol/phenolate equilibrium were carried out in organic solvents using organic bases for deprotonation. The spectra of **BODIPY–OH** in different solvents containing butylamine (BA), 1,5-diazabicyclo[4.3.0]non-5-ene (DBN), and 1,8-diazabicyclo[5.4.0]undec-7-ene (DBU) are shown in Fig. 3–4 and Fig. S3–S6†.

In the presence of the weaker base BA, two kinds of spectra characteristics can be inspected. In nearly nonpolar solvents, such as benzene, addition of BA results in the appearance of a small red-shifted (9 nm) absorption band (Fig. 3 and Fig. S3†), indicating the weak hydrogen-bonded interaction between **BODIPY–OH** and BA. Accordingly, the emission spectrum exhibits weak solvatochromism, and the emission band comes from (**BODIPY–OH**)* excited state with 10 nm bathochromic shift. Inspection of the spectra characteristics in polar solvents shows that **BODIPY–OH** exists as mixtures with varying ratios of the phenol and phenolate, the exception is in water and DMSO in the presence of BA (Fig. S5†); in water and DMSO, only **BODIPY–O**$^-$ is generated. Fluorescence of **BODIPY–O**$^-$ together with **BODIPY–OH** is observed upon excitation of **BODIPY–OH** (Fig. 4). Excitation of the phenol form results in partial conversion of (**BODIPY–OH**)* to (**BODIPY–O**$^-$)*, followed by emission from the ion, thus a relatively large Stokes shift (~70 nm in protic solvents and ~90 nm in CH_3CN and DMF) and a secondary, weak emission is observed.

In contrast, the absorption profiles of **BODIPY–OH** on addition of stronger bases DBN or DBU change drastically, and the absorption band of the neutral phenol form is replaced by that of a hydrogen-bonded complex (HBC) of **BODIPY–OH** with

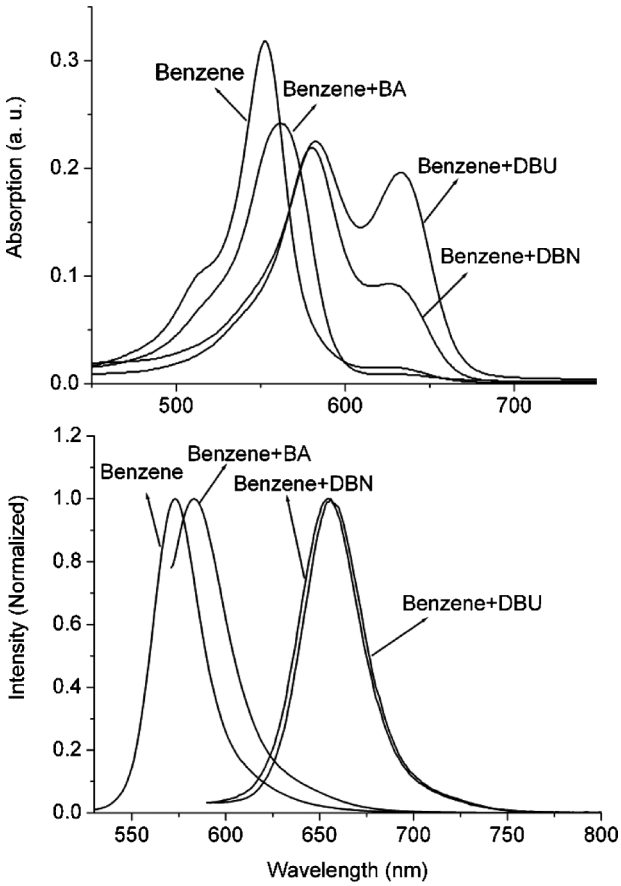

Fig. 3 UV-vis absorption (top) and fluorescence spectra (bottom) of **BODIPY–OH** (5.0×10^{-6} M) in benzene containing no and organic bases (0.010 M).

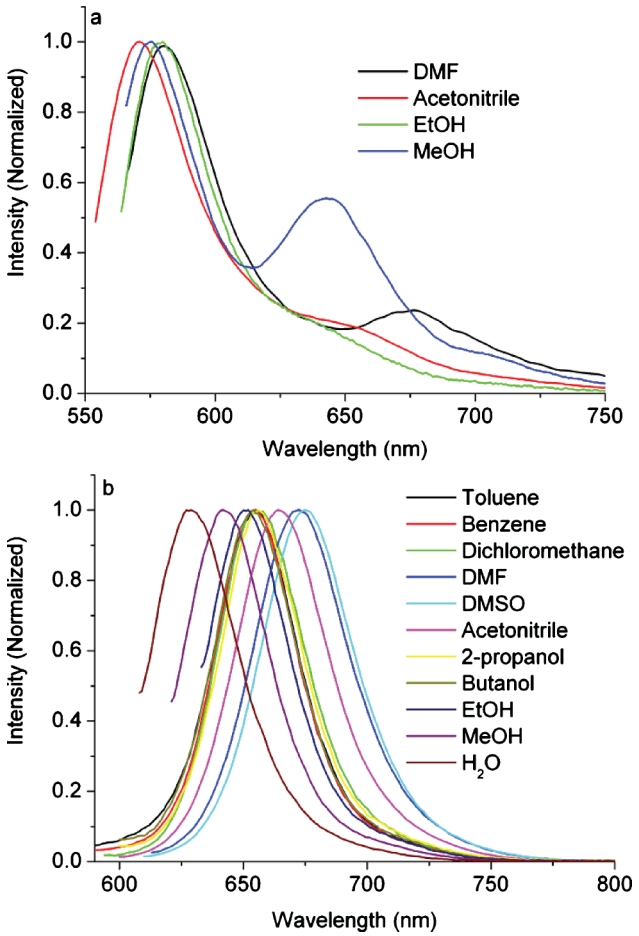

Fig. 4 Fluorescence spectra of **BODIPY–OH** (5.0×10^{-6} M) (top) in solutions containing BA base recorded at the first excitation wavelength. (λ_{ex} = 556 nm for DMF, 542 nm for acetonitrile, 554 nm for EtOH and 553 nm for MeOH). In the presence of DBN (0.010 M) in various solvents (bottom).

the bases and/or that of **BODIPY–O**$^-$ with the conjugate acids of organic bases (*i.e.*, H-DBN$^+$ and H-DBU$^+$) which behave as countercations for **BODIPY–O**$^-$. In benzene or toluene, upon addition of either of DBN and DBU, a red-shifted absorption band of phenolate ion is observed accompanied by the absorption band of HBC of **BODIPY–OH** with the bases (Fig. 3). In the two cases, selective excitation of either **BODIPY–OH** in an HBC or **BODIPY–O**$^-$ results in emission exclusively from (**BODIPY–O**$^-$)* at λ_{em} ~656 nm. The fluorescence maximum of **BODIPY–O**$^-$ from HBC shows a relatively large Stokes shift (~80 nm). This result indicates that (**BODIPY–OH**)* in an HBC gives the excited state of (**BODIPY–O**$^-$)* by proton transfer, a well-known mechanism for fluorescence of a phenol derivative making an HBC with organic bases in a less polar solvents.[14] Although the Stokes shift is not greater than 100 nm, it is still a significant improvement when compared to a typical Stokes shift of BODIPYs, which is always 2 ~ 3 times smaller than that reported here. In solvents that are more polar than dichloromethane (E_T (N) = 0.309), **BODIPY–OH** is completely ionized at the ground state, and the phenolate form exists exclusively. As a consequence, the fluorescence spectrum of **BODIPY–O**$^-$, generated by direct excitation of the phenolate form, shows a small Stokes shift like that of typical BODIPYs.

It is worth noting that both **BODIPY–OH** and **BODIPY–O**$^-$ display emission with high quantum yield in different solvents (Table 1 and Table S2†). In particular, the quantum yield of the anion form is in the range 0.17 ~ 0.24, which is much larger compared to that of reported BODIPYs bearing phenolic subunits. The reported examples usually have very low quantum yields.

Fig. 4 shows the solvent-dependent emissions of **BODIPY–O**$^-$. The λ_{em} values range from 629 ~ 681 nm, and are modulated only by the polarity of the enviroment, while the emission maximum is bathochromic shifted by 3 ~ 5 nm from solutions containing DBN to DBU. The variation of λ_{em} values for **BODIPY–OH** in studied solvents containing DBN is evaluated by correlating the emission maxima (λ_{em}) with the normalized Dimroth–Reichardt's solvent parameter E_T(N) (Fig. 5).[15] The plot shows two distinct regions, one is in the E_T(N) range from 0.099 to 0.444 for less polar solvents and the other in the E_T(N) range from 0.444 to 1.000 for polar solvents. In the region for less polar solvents, the emission maxima shows positive solvatochromism (increasing λ_{em} with E_T(N)), and the lowest energy emission is from **BODIPY–O**$^-$ in DMSO. With increasing polarity of solvents into the polar region, the emission maxima shows negative solvatochromism. It is worth noting that the plot is a straight line with respect to E_T(N) in protic solvents, represented by the equation $\lambda_{em} = -63.5\ E_T(N) + 691.6$ (r = 0.996). The negative slope and the longest emission wavelength of **BODIPY–O**$^-$ in DMSO indicate that increasing

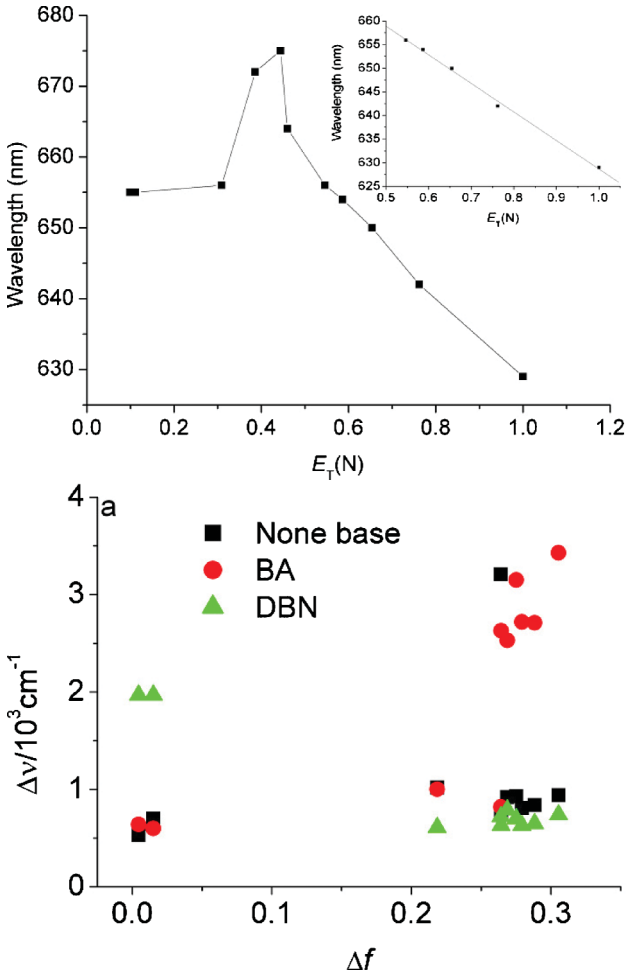

Fig. 5 Emission maxima (top) (λ_{em}) plotted as function of E_T(N). Inset: the linear correlation of λ_{em} with E_T(N) in protic solvents. Lippert–Mataga plot (bottom) of the solvent effects on the spectra of **BODIPY–OH** in the absence and presence of base.

polarity is not favorable for tuning the color to the red region, and the optimum condition for achieving the strongest red shift of the emission is in DMSO with bases.

To get an insight into the solvatochromic behaviors of enol and enolate forms, the Stokes shift as a function of orientational polarizability (Δf) was studied using the Lippert–Mataga model.

$$\Delta\overline{V} = \frac{2\Delta f}{4\pi\varepsilon_0 hca^3}(\mu_e - \mu_g)^2 + \text{constant} \quad (3)$$

where

$$\Delta f = \left(\frac{\varepsilon - 1}{2\varepsilon - 1} - \frac{n^2 - 1}{2n^2 + 1}\right) \quad (4)$$

In the equations, a represents the radius of the cavity in which the fluorophore resides. μ_g and μ_e denote the dipole moments in the ground and excited states, respectively. Deviation from the linearity is usually an indication of the presence of a specific interaction other than a simple dipole–dipole interaction. In our system, an analysis of the Stokes shifts with Lippert–Mataga equation gives strong deviation from linear correlation, indicating significant effects of specific interactions and, particularly, hydrogen bonding on the energy of **BODIPY–OH*** (Fig. 5).[16]

Conclusions

In this paper, we have described the synthesis and systemic study of the spectroscopic characteristics of **BODIPY–OH** and **BODIPY–O**$^-$ in various solvents containing an organic base. The straightforward phenol/phenolate interconversion induces dramatic changes in absorption and emission spectra. The spectra of **BODIPY–O**$^-$ vary depending on the environment polarity with the wavelength finely tunable over a wide range. λ_{em} values of **BODIPY–O**$^-$ can be modulated in the range 629 to 681 nm by the polarity of solvents, while λ_{em} values of **BODIPY–OH** are in the range 571 to 586 nm. These results demonstrate that the color of the solution can be tuned, over a range of 110 nm, by converting the phenol form of **BODIPY–OH** to the phenolate form, which is caused by changing the environmental polarity in the vicinity of **BODIPY–OH**. Furthermore, the fluorescence of **BODIPY–O**$^-$ with high quantum yield shows relatively large Stokes shift in solvent/base combinations, accomplished by excited state deprotonation from (**BODIPY–OH**)* to (**BODIPY–O**$^-$)*, suggesting it is more suitable for use as a fluorescent probe in bioassays.

Experimental

General methods

All chemical reagents and solvents for synthesis were purchased from commercial suppliers and were used without further purification. All moisture-sensitive reactions were carried out under an atmosphere of argon. ^{1}H NMR and ^{13}C NMR spectra were recorded on a Bruker AV-400 spectrometer with chemical shifts reported in ppm (in $CDCl_3$, TMS as internal standard) at room temperature. Mass spectra were measured on a HP 1100 LC-MS spectrometer.

Synthesis

BODIPY–OH. To a solution of 2-benzoyl-3-methyl-6-methoxyindole (1 g, 3.76 mmol) in CH_2Cl_2 (60 mL) was added $POCl_3$ (1.05 mL, 11.28 mmol) at 0 °C, the resulting solution was stirred for a further 5 min, followed by addition of 2,4-dimethyl-3-ethylpyrrole. The mixture was warmed to room temperature and stirred for 3 days, cooled to 0 °C, neutralized with saturated Na_2CO_3, and washed with H_2O. The organic phase was dried with Na_2SO_4, and the solvent was removed to obtain a dark oil. To the resulting oil in anhydrous CH_2Cl_2 was added BBr_3 (3.48 mL, 37.6 mmol) at −15 °C. The reaction mixture was stirred for a further 1 h at −15 °C, then warmed to room temperature, quenched with H_2O, extracted with CH_2Cl_2, and washed with H_2O. The combined organic extracts were dried with Na_2SO_4, and Na_2SO_4 was removed by filtration. Then Et_3N (5.6 mL) was added to the solution at room temperature, and the resulting mixture was stirred for 5 min, cooled to 0 °C, followed by addition of $BF_3{\cdot}OEt_2$, and stirred for another 30 min. The reaction mixture was extracted with CH_2Cl_2, washed with H_2O, dried over Na_2SO_4, and the solvent was removed *in vacuo*. The crude product was purified by flash chromatography (silica gel, eluent: CH_2Cl_2 then EtOAc/CH_2Cl_2 1 : 10) to obtain 800 mg (53%) **BODIPY–OH**: ^{1}H NMR (400 MHz, $CDCl_3$) δ 1.03 (t, 3H), 1.40 (s, 3H), 1.60 (s, 3H), 2.35–2.41 (q, 2H), 2.69 (s, 3H),

6.61–6.65 (dd, 1H), 7.1 (m, 1H), 7.34–7.37 (m, 3H), 7.54–7.56 (m, 3H); ^{13}C NMR (100 MHz, $CDCl_3$) δ 161.8, 157.7, 146.5, 141.6, 141.5, 136.8, 135.3, 133.3, 132.7, 129.3, 129.1, 128.3, 127.0, 122.7, 112.4, 98.7, 17.2, 14.2, 13.4, 12.2, 11.3; HRMS (ESI) Calcd for $C_{24}H_{22}BF_2N_2O$: 403.1793. Found: 403.1825. $[M - H]^-$.

BODIPY–OMe. To a solution of 2-benzoyl-3-methyl-6-methoxyindole (1 g, 3.76 mmol) in CH_2Cl_2 (60 mL) was added $POCl_3$ (1.05 mL, 11.28 mmol) at 0 °C, the resulting solution was stirred for a further 5 min, and was followed by the addition of 2,4-dimethyl-3-ethylpyrrole. The resulting mixture was warmed to room temperature and stirred for 3 days, cooled to 0 °C, neutralized with saturated Na_2CO_3, and washed with H_2O. The organic phase was dried with Na_2SO_4, and the solvent was removed to obtain a dark oil. To the resulting oil in anhydrous CH_2Cl_2 was added Et_3N (5.6 mL) at room temperature, and the mixture was stirred for 5 min, cooled to 0 °C, followed by addition of $BF_3{\cdot}OEt_2$, and stirred for another 30 min. The reaction mixture was extracted with CH_2Cl_2, washed with H_2O, dried over Na_2SO_4, and the solvent was removed *in vacuo*. The crude product was purified by flash chromatography (silica gel, eluent: hexane/CH_2Cl_2 1 : 1) to obtain 1.03 g (66%) **BODIPY–OMe**: ^{1}H NMR (400 MHz, $CDCl_3$) δ 1.02 (t, 3H), 1.38 (s, 3H), 1.57 (s, 3H), 2.39–2.33 (q, 2H), 2.67 (s, 3H), 3.94 (s, 3H), 6.65–6.61 (dd, 1H), 7.11 (d, 1H), 7.30 (d, 1H), 7.35–7.32 (m, 2H), 7.64–7.52 (m, 3H); ^{13}C NMR (100 MHz, $CDCl_3$) δ 162.1, 161.0, 147.1, 141.6, 141.3, 136.5, 135.4, 133.2, 132.9, 129.3, 129.1, 128.3, 128.1, 126.8, 122.2, 113.9, 94.9, 55.6, 17.2, 14.3, 13.3, 12.1, 11.3; HRMS (ESI) Calcd for $C_{25}H_{24}BF_2N_2O$: 417.1950. Found: 417.1938. $[M - H]^-$.

Acknowledgements

We gratefully acknowledge the financial support of the National Science Foundation of China (Grant no.: 20902021) and the Scientific Research Foundation for Returned Overseas Chinese Scholars (State Education Ministry).

Notes and references

1 (*a*) R. Ziessel, G. Ulrich and A. Harriman, *New J. Chem.*, 2007, **31**, 496–501; (*b*) A. Loudet and K. Burgess, *Chem. Rev.*, 2007, **107**, 4891–4932; (*c*) G. Ulrich, R. Ziessel and A. Harriman, *Angew. Chem. Int. Ed.*, 2008, **47**, 1184–1201.
2 (*a*) M. Baruah, W. Qin, N. Basarić, W. M. De Borggraeve and N. Boens, *J. Org. Chem.*, 2005, **70**, 4152–4157; (*b*) W. Qin, M. Baruah, M. Van der Auweraer, F. C. De Schryver and N. Boens, *J. Phys. Chem. A*, 2005, **109**, 7371–7384; (*c*) M. Baruah, W. Qin, C. Flors, J. Hofkens, R. A. L. Vallée, D. Beljonne, M. Van der Auweraer, W. M. De Borggraeve and N. Boens, *J. Phys. Chem. A*, 2006, **110**, 5998–6009; (*d*) W. Qin, M. Baruah, M. Sliwa, M. Van der Auweraer, W. M. De Borggraeve, D. Beljonne, B. Van Averbeke and N. Boens, *J. Phys. Chem. A*, 2008, **112**, 6104–6114.
3 (*a*) K. Umezawa, Y. Nakamura, H. Makino, D. Citterio and K. Suzuki, *J. Am. Chem. Soc.*, 2008, **130**, 1550–1551; (*b*) K. Umezawa, A. Matsui, Y. Nakamura, D. Citterio and K. Suzuki, *Chem. Eur. J.*, 2009, **15**, 1096–1106; (*c*) T. Bura, P. Retailleau, G. Ulrich and R. Ziessel, *J. Org. Chem.*, 2011, **76**, 1109–1117.
4 (*a*) L. Tolosa, K. Nowaczyk, J. Lakowicz, *An Introduction to Laser Spectroscopy*, 2nd ed.; Kluwer: New York, 2002; (*b*) X. Peng, F. Song, E. Lu, Y. Wang, W. Zhou, J. Fan and Y. Gao, *J. Am. Chem. Soc.*, 2005, **127**, 4170–4171.
5 (*a*) K. M. Solntsev, O. Poizat, J. Dong, J. Rehault, Y. Lou, C. Burda and L. M. Tolbert, *J. Phys. Chem. B*, 2008, **112**, 2700–2711; (*b*) J. Dong, F. Abulwerdi, A. Baldridge, J. Kowalik, K. M. Solntsev and L. M. Tolbert, *J. Am. Chem. Soc.*, 2008, **130**, 14096–14098; (*c*) M. Chattoraj, B. A. King, G. U. Bublitz and S. G. Boxer, *Proc. Natl. Acad. Sci. USA*, 1996, **93**, 8362–8367.
6 (*a*) C. Fang, R. R. Frontiera, R. Tran and R. A. Mathies, *Nature*, 2009, **462**, 200–204; (*b*) M. W. Forbes and R. A. Jockusch, *J. Am. Chem. Soc.*, 2009, **131**, 17038–17039.
7 (*a*) N. N. Ugarova, *Photochem. Photobiol. Sci.*, 2008, **7**, 218–227; (*b*) V. R. Viviani, F. G. C. Arnoldi, A. J. S. Neto, T. L. Oehlmeyer, E. J. H. Bechara and Y. Ohmiya, *Photochem. Photobiol. Sci.*, 2008, **7**, 159–169.
8 (*a*) Y. Ando, K. Niwa, N. Yamada, T. Enomoto, T. Irie, H. Kubota, Y. Ohmiya and H. Akiyama, *Nat. Photonics*, 2008, **2**, 44–47; (*b*) T. Nakatsu, S. Ichiyama, J. Hiratake, A. Saldanha, N. Kobashi, K. Sakata and H. Kato, *Nature*, 2006, **440**, 372–376.
9 (*a*) B. R. Branchini, M. H. Murtiashaw, R. A. Magrar, N. C. Portier, M. C. Ruggiero and J. G. Stroh, *J. Am. Chem. Soc.*, 2002, **124**, 2112–2113; (*b*) I. Navizet, Y.-J. Liu, N. Ferré, H.-Y. Xiao, W.-H. Fang and R. Lindh, *J. Am,. Chem. Soc.*, 2010, **132**, 706–712.
10 T. Hirano, Y. Hasumi, K. Ohtsuka, S. Maki, H. Niwa, M. Yamaji and D. Hashizume, *J. Am. Chem. Soc.*, 2009, **131**, 2385–2396.
11 (*a*) P. Naumov and M. Kochunnoonny, *J. Am. Chem. Soc.*, 2010, **132**, 11566–11579; (*b*) P. Naumov, Y. Ozawa, K. Ohkubo and S. Fukuzumi, *J. Am. Chem. Soc.*, 2009, **131**, 11590–11605.
12 (*a*) J. Murtagh, D. O. Frimannsson and D. F. O'Shea, *Org. Lett.*, 2009, 5386–5389; (*b*) A. Coskun, E. Deniz and E. U. Akkaya, *Org. Lett.*, 2005, 5187–5189; (*c*) T. Gareis, C. Huber, O. S. Wolfbeis and J. Daub, *Chem. Commun.*, 1997, 1717–1718.
13 T. Z. Förster, *Elektrochem. Ber. Bunsen-Ges. physik. Chem.*, 1950, **54**, 42.
14 (*a*) L. M. Tolbert and S. M. Nesselroth, *J. Phys. Chem.*, 1991, **95**, 10331–10336; (*b*) K. J. Willis and A. G. Szabo, *J. Phys. Chem.*, 1991, **95**, 1585–1589.
15 (*a*) C. Reichardt, *Chem. Rev.*, 1994, **94**, 2319–2358; (*b*) C. Reichardt, In *Solvents and Solvent Effects in Organic Chemistry*, 3rd ed.; Wiley-VCH: Weinheim, Germany, 2003.
16 (*a*) E. Z. Lippert, *Electrochem.*, 1957, **61**, 962; (*b*) N. Mataga, Y. Kaifu and M. Koizumi, *Bull. Chem. Soc. Jpn.*, 1956, **29**, 465.

